



Fermi National Accelerator Laboratory

FERMILAB-Pub-80/44-EXP
7420.180

(Submitted to Nucl. Phys. B)

CHARGED CURRENT EVENTS WITH NEUTRAL STRANGE PARTICLES IN HIGH ENERGY ANTINEUTRINO INTERACTIONS

V. V. Ammosov, A. G. Denisov, P. F. Ermolov, G. S. Gapienko,
V. A. Gapienko, V. I. Klukhin, V. I. Koreshev, P. V. Pitukhin,
V. I. Sirotenko, E. A. Slobodyuk, Z. V. Usubov, and V. G. Zaetz
Institute of High Energy Physics, Serpukhov, USSR

and

J. P. Berge, D. Bogert, R. Endorf, R. Hanft, J. A. Malko,
G. I. Moffatt, F. A. Nezrick, R. Orava, and J. Wolfson
Fermi National Accelerator Laboratory
Batavia, Illinois 60510 USA

and

V. I. Efremenko, A. V. Fedotov, P. A. Gorichev, V. S. Kaftanov,
G. K. Kliger, V. Z. Kolganov, S. P. Krutchinin, M. A. Kubantsev,
I. V. Makhljueva, V. I. Shekeljan, and V. G. Shevchenko
Institute for Theoretical and Experimental Physics, Moscow, USSR

and

J. Bell, C. T. Coffin, B. P. Roe, A. A. Seidl, D. Sinclair,
and E. Wang
University of Michigan, Ann Arbor, Michigan 48104 USA

May 1980



ABSTRACT

The results of a study of strange particle production in charged current $\bar{\nu}_\mu N$ interactions in the Fermilab 15-Ft. bubble chamber filled with a heavy Ne-H₂ mixture are presented. Production rates and average multiplicities of K⁰'s and Λ 's as functions of w^2 and Q^2 are given. The experimental data agrees well with the quark-parton model predictions if a relative yield of 0.06 ± 0.02 of K⁰'s and Λ 's from the charm production is included. Upper limits for the D meson production are given and the shape of the charmed quark fragmentation function is discussed. Inclusive production of the K^{*} (890) and Σ (1385) resonances is considered and it is shown that only about 5% of the K⁰ mesons and Λ hyperons results from the resonance decays. Relative production rates of neutral strange particles on proton and neutron targets are studied.

I. INTRODUCTION

Strange particles produced by lepton beams can be used as a probe for the production of charmed particles. Since in the GIM charm-scheme¹ the charm-to-strange quark transition is favoured we expect to see a reflection of charm production in the events with strange particles in their final states. Non-leptonic decays of charmed particles have already been recorded in e^+e^- storage ring experiments², photoproduction experiments³ and $\bar{\nu}N$ experiments⁴. Signals for semi-leptonic charmed particle decays in $\bar{\nu}N$ interactions have been reported by us in a previous study of μe events⁵. The quark-parton model (QPM)⁶ predicts that essentially all the charmed particle production in $\bar{\nu}N$ interactions is off of sea quarks, and therefore, a study of the scaling variable distributions for inclusive strange particle production can be expected to give indications of charm production⁷.

In this paper the results of an investigation of K^0 mesons and Λ hyperons produced in high energy charged current (CC) antineutrino-nucleon interactions are presented. The inclusive momentum spectra of neutral strange particles observed in this experiment have been published earlier⁸. Here we consider production rates, average multiplicities, the effects of charmed particle production and the production of the resonances K^* (890) and Σ (1385). Finally, we discuss the relative rates of neutral strange particles produced in interactions with proton and neutron target.

II. EXPERIMENTAL DETAILS

The data analysis is based on charged current antineutrino events obtained in the Fermilab 15-Ft. bubble chamber filled with a 36% H_2 -64%Ne atomic mixture exposed to a wide-band antineutrino beam. A total of 85,000 pictures were taken in the double-horn focused beam with plug and 70,000 pictures with a bare target sign selected antineutrino beam. The incident proton energy was 400 GeV.

The film was scanned for all neutral-induced interactions with two or more prongs. About 23,000 events were fully measured and processed through the geometrical reconstruction program. The scan efficiency was measured in a partial double scan and a multiplicity dependent weight was assigned to every event. The scan efficiency varies from 65% for the two-prong events up to $\sim 100\%$ for the events with multiplicity greater than six.

Muons were identified by the External Muon Identifier supplemented by a large-transverse momentum procedure. The overall efficiency for muon identification was $\sim 92\%$ independent of angle for muons with momentum greater than 4 GeV/c.⁹ The energy of the incident antineutrino was estimated using an average correction for neutral energy loss characteristic of the total sample of events from this experiment.¹⁰ Finally, the total CC event sample was required to (a) have a positive muon with momentum greater than 4 GeV/c, (b) be in a restricted fiducial volume ($\sim 17m^3$) and (c) have the incident antineutrino energy larger than 10 GeV. The number of antineutrino CC events passing these cuts was about 8200 events.

A subsample of V^0 charged current events was defined in the following way. Events having one or more candidates for the decays $K_S^0 \rightarrow \pi^+ \pi^-$, $\Lambda \rightarrow p \pi^-$ or $\bar{\Lambda} \rightarrow \bar{p} \pi^+$ associated with the primary vertex were processed through the kinematics fitting program. Details of the V^0 analysis are given in Ref. 8. Each V^0 was then weighted to account for the geometrical detection inefficiency, neutral decay modes (including lost K_L^0 's) and scanning and processing inefficiencies. The average weights obtained were 3.9 for K_S^0 , 2.0 for Λ and 2.2 for $\bar{\Lambda}$. Observed raw and corrected numbers of the V^0 CC events in various channels are given in Table I. Since charged strange particles are not effectively identified, the various K^0 and Λ channels contain contributions from the associated production of neutral strange particles with the charged ones.

III. EXPERIMENTAL RESULTS

3.1 Production rates and average multiplicities

The total number of charged current V^0 events corrected for the experimental inefficiencies, decay modes and potential-length selections is equal to 1320 ± 79 events. Normalized to the total CC event sample this leads to a total V^0 event rate of 0.16 ± 0.01 for $E_{\bar{\nu}} > 10$ GeV. Event rates for various V^0 channels are given in Table I. For inclusive yields of K^0 and Λ we have:

$$R_K = (\bar{\nu}N \rightarrow \mu^+ K^0 X) / (\bar{\nu}N \rightarrow \mu^+ X) = 0.164 \pm 0.009$$

$$R_\Lambda = (\bar{\nu}N \rightarrow \mu^+ \Lambda X) / (\bar{\nu}N \rightarrow \mu^+ X) = 0.063 \pm 0.004$$

$$R_{\Lambda/K} = (\bar{\nu}N \rightarrow \mu^+ \Lambda X) / (\bar{\nu}N \rightarrow \mu^+ K^0 X) = 0.38 \pm 0.03$$

These rates are compared to the strange particle yields obtained in other neutrino and antineutrino experiments in Table II.

Since the charged K 's are not identified it is not possible to determine the single strange particle production rate in our data. However, we may estimate the number of $\Delta S = \Delta Q$ events which contain a Λ by assuming equal rates for the ΛK^0 and ΛK^+ (associated) production. With this assumption we obtain the Λ production rate in the $\Delta S = \Delta Q$ processes of $(1.1 \pm 0.7)\%$ of the total CC sample. This value is compatible with the QPM predictions of $\sim 4\%$ for the total single strange particle production in $\bar{\nu}N$ interactions obtained using our experimental conditions and the quark densities of Ref. 17.

In principle, the average strange particle multiplicities may be functions of both W^2 and Q^2 , where W is the total hadronic invariant mass and Q^2 is the square of the four-momentum transfer between the incident antineutrino and the outgoing muon. The W^2 dependence of the K^0 and Λ multiplicity is shown in Fig. 1(a,b). For comparison, data from neutrino-nucleon¹¹ charged current interactions are also plotted in these figures. A strong rise with W^2 is seen for both K^0 and Λ multiplicities and a logarithmic parametrisation of the data over the range $2 < W^2 < 200 \text{ GeV}^2$ for K^0 's and $2 < W^2 < 100 \text{ GeV}^2$ for Λ 's yields

$$\langle n_K \rangle = (-0.068 \pm 0.017) + (0.094 \pm 0.009) \ln W^2$$

$$\langle n_\Lambda \rangle = (0.008 \pm 0.012) + (0.024 \pm 0.005) \ln W^2$$

with $\chi^2/\text{ND}=17.4/10$ for K^0 and $\chi^2/\text{ND}=7.5/9$ for Λ data. A fit to the expression $\langle n \rangle = a + bW^{1/2}$ (Ref. 16) gives the following results

$$\langle n_K \rangle = (-0.250 \pm 0.033) + (0.220 \pm 0.021) W^{1/2}$$

$$\langle n_\Lambda \rangle = (-0.029 \pm 0.019) + (0.052 \pm 0.011) W^{1/2}$$

with $\chi^2/\text{ND}=13.0/10$ for K^0 and $\chi^2/\text{ND}=7.7/9$ for Λ data, respectively. It is apparent that the behaviour of $\langle n_K \rangle$ and $\langle n_\Lambda \rangle$ is similar for both $\bar{\nu}N$ and νN data.

In Fig. 1a we also present the W^2 dependence of $\langle n_K \rangle$ for K^0 mesons with $z > 0.3$ where z is defined for an individual hadron h by $z = E_h/\nu$ where E_h is the energy of hadron h , ν is the total hadronic energy in the laboratory system. This selection is applied to remove most K^0 's associated with the target fragmentation region. We can see that there is no clear dependence of $\langle n_K \rangle$ on W^2 . This is in agreement with the νp data in the current fragmentation region¹⁴.

In Fig. 2 we show the neutral strange particle multiplicities as a function of Q^2 . The K^0 and Λ data give indication of a slow increase in the mean multiplicity with the increasing Q^2 . The increase might be related to the strong W^2 dependence of the V^0 multiplicities as observed above. To check this we present the values of $\langle n_K \rangle$ and $\langle n_\Lambda \rangle$ as a function of Q^2 in Fig. 3(a,b) for two W^2 regions: $W^2 < 20 \text{ GeV}^2$ and $W^2 > 20 \text{ GeV}^2$. With these W^2 selections no significant dependence of $\langle n_V \rangle$ on Q^2 is observed.

The behaviour of the mean K^0 multiplicity in the current fragmentation region ($z > 0.3$) is shown in Fig. 2a by open data points. Within the limits of statistics, our experimental data are consistent with no dependence of Q^2 in agreement with the νp data¹⁴. The absence of a Q^2 dependence is expected in the quark-parton picture of quark fragmentation.

3.2 Indirect search for charm effects

In the QPM the main part of the antineutrino-nucleon cross section comes from valence quark scattering and the cross section therefore has a y -dependence, $d\sigma/dy \sim (1-y)^2$. On the other hand, charm production occurs only off sea antiquarks and should be concentrated at low x and have a flat y -distribution. Here x and y are the usual Bjorken scaling variables ($x = Q^2/2M\nu$, $y = \nu/E_\nu$). Since charmed particles decay primarily into strange particles, one can use strange particles as charm triggers. Then one can look for an excess of K^0 's and Λ 's with respect to the ordinary single and associated strange particle production at low x and large y . The inclusive particle spectra integrated over x and y , on the other hand, are expected to be insensitive to the effects from charm production.

The antineutrino charged current differential cross section off an isoscalar target can be written in the QPM as

$$\sigma_1(x,y) \sim (u+d)(1-y)^2 + (\bar{u}+\bar{d}+2\bar{s})$$

where u , d , \bar{u} ,... are the quark densities $xu(x)$, $xd(x)$, $x\bar{u}(x)$,... for the corresponding quarks in a proton, as given in Ref. 17 (we neglect the contribution of charmed quarks in the sea). Thus, we can identify the various contributions to the total $V^0(K^0 \text{ and } \Lambda)$ production as

(a) Non-charm single V^0 production, σ_2

$$\sigma_2(x,y) \sim \sin^2\theta_C \{(u+d)(1-y)^2 + 2\bar{s}\}$$

where the first term comes from the $u \rightarrow s$ transition and the second term from the $\bar{s} \rightarrow \bar{u}$ transition (the V^0 is then combined from the left-over s quark in the $s\bar{s}$ pair).

(b) Charm-induced V^0 production, σ_3

$$\sigma_3(x,y) \sim \sin^2\theta_C (\bar{u}+\bar{d}) + 4\bar{s} \cos^2\theta_C$$

where the first term comes from the $\bar{d} \rightarrow \bar{c}$ transition and the second from the $\bar{s} \rightarrow \bar{c}$ transition (a factor 4 appears because in this case we expect two strange particles: one from the charmed particle decay and another from an s quark in the sea).

(c) Finally, we must include the associated $s\bar{s}$ production. We assume that this cross section, σ_4 , can be written as a product of two terms, one which has the same x and y dependence as the total CC cross section σ_1 , and one which has a logarithmic W^2 dependence, i.e.

$$\sigma_4(x, y) \sim \sigma_1(x, y) \{ a + b \cdot \ln W^2 \}$$

The parameters a and b were taken from the K^0 and Λ production in non-weak processes¹⁰. The final results are not strongly affected by the choice of these parameters.

Then we introduce a set of functions of the scaling variables, x and y

$$f_i(t) = \iint \sigma_i(t, t') E \phi(E) \theta_i(E, t, t') dE dt'$$

$$F_i(t) = f_i(t)/f_1(t); \quad i=1$$

$$\int f_i(t) dt = 1; \quad i=1, 2, \dots, 4$$

where t is either x or y (t' is either y or x). Here $\phi(E)$ is the relative antineutrino flux obtained from our CC data and θ_i are the step-functions which take into account the experimental selections and threshold effects.

We can now write the ν^0 multiplicity in the following form:

$$\frac{dN(\nu^0)/dt}{dN(CC)/dt} = \langle n_2^V \rangle F_2(t) + \langle n_3^V \rangle F_3(t) + \langle n_4^V \rangle F_4(t)$$

where $N(V^0)$ and $N(CC)$ are the numbers of V^0 's and charged current events, respectively, and $\langle n_i^V \rangle$ is the partial average V^0 multiplicity from the production source i , integrated over entire x and y regions. We have used the above expressions to make a simultaneous fit to our experiment x - and y - distributions. The results are shown in Fig. 4a and 4b, where the solid lines represent the results of the complete fit and the dashed lines show the non-charm part of the fit. Because the shapes of functions F_2 and F_4 are very similar in the central regions of x and y , the average V^0 multiplicity from the single production $\langle n_2^V \rangle$, was used as a fixed parameter. The value used was obtained with an assumption that the charged and neutral kaons are produced with an equal probability and that the number of Λ 's and Σ^0 's is approximately equal to the number of Σ^\pm 's. The QPM then gives, with these assumptions, $\langle n_2^V \rangle = 0.021$.

The fit with the charm term gives a value of $\chi^2/ND=21.0/17$ which corresponds to a probability of $P(\chi^2) = 23\%$. This result should be compared with $P(\chi^2) \sim 10^{-4}$ which was obtained by fitting the data to the same form without the charm term. Thus we see that the observed behaviour of the average V^0 multiplicity as a function of x and y can be described by the QPM where the charmed quarks are produced off sea quarks and decay into strange particles according to the GIM mechanism.

The fit predicts that the total charm contribution to the K^0 and Λ multiplicity is

$$\langle n_3^V \rangle = 0.06 \pm 0.02$$

If we assume that the K^0 's and Λ 's represent about one half of the total strange particle production rate, the total average strange particle multiplicity due to charm is $2 \cdot 0.06$. Finally, since charm production results in two strange particles per event, we multiply the strange particle multiplicity by $1/2$ to obtain the charm contribution of 0.06 ± 0.02 to the total charged current cross section. This 6% is compatible with the observed μ^+e^- rate in this experiment⁵.

3.3 Charm fragmentation

Models describing hadron production in the deep-inelastic reactions are based on the idea of quark fragmentation⁷. To obtain predictions for the strange particle production in these models one has to know the shape of charmed quark fragmentation functions. Here we use our data on inclusive K^0 production in the high z region ($z > 0.3$) and compare them with the QPM predictions.

The inclusive K^0 cross section for the current fragmentation region ($z > 0.3$) is given in the QPM as

$$\begin{aligned} \frac{d^3\sigma}{dx dy dz} = & \frac{G_{ME}^2}{s} \{ (u+d) (1-y)^2 [\cos^2\theta_c D_d^K(z) + \sin^2\theta_c D_s^K(z)] + \\ & + (\bar{u}+\bar{d}) [\cos^2\theta_c D_u^K(z) + \sin^2\theta_c D_c^K(z)] + \\ & + 2\bar{s} [\cos^2\theta_c D_c^K(z) + \sin^2\theta_c D_u^K(z)] \} \end{aligned}$$

where $u, d, \dots \bar{s}$ are quark densities (see Sec. 3.2), $D_q^K(z)$ is the fragmentation function of a quark q into the K^0 meson and θ_C is the Cabibbo angle. Our data do not allow us to determine the four fragmentation functions in the above formula. However, in the region $x > 0.3$ the antiquark densities are negligible. Normalizing to the total charged current sample, we have for the region $x > 0.3$.

$$\frac{1}{N_{CC}} \frac{dn}{dz} = \cos^2 \theta_C D_d^K(z) + \sin^2 \theta_C D_s^K(z)$$

where N_{CC} is the number of charged current events and n is the number of K^0 mesons.

Using our data in the region $x > 0.3$, $z > 0.3$ we obtain

$$\int_{0.3}^1 [\cos^2 \theta_C D_d^K(z) + \sin^2 \theta_C D_s^K(z)] dz = 0.068 \pm 0.011$$

This number agrees well with the value of ~ 0.075 deduced from the measurements of $D_d^K(z)$ and $D_s^K(z)$ in a recent ep experiment¹⁹.

Next we use our inclusive K^0 data to search for the effects of charmed particle production. The z -distribution of the K^0 's obtained by integrating the differential cross section over the entire x and y region is not sensitive to the charm term. This insensitivity is due to the only $\sim 10\%$ over-all contribution from sea antiquarks in the total cross section. Therefore, we have studied the inclusive K^0 yield as a function of x and y in the current fragmentation region ($z > 0.3$).

For the term $\cos^2 \theta_C D_d^K + \sin^2 \theta_C D_s^K$ we use the result obtained above from our data and for the $D_U^K(z)$ fragmentation function we take the function determined in an ep experiment¹⁹. The only unknown quantity is then the charmed quark fragmentation function $D_C^K(z)$. This function should describe a two-step process where the charmed quark first dresses itself into a charmed particle. The charmed particle then decays into the observed final-state hadrons. For our calculations we have assumed that these intermediate charmed particles are all D(1860) mesons, D^- or \bar{D}^0 , and that the observed K^0 mesons come from the subsequent D(1860) decays.

Calculation of the charmed quark fragmentation function, $D_C^K(z)$ is related to the knowledge of the fragmentation function for a charmed quark into the D (1860) mesons, $D_C^D(z')$, where z' is the fractional hadronic energy of the charmed meson, and the decay kinematics for the various $D(1860) \rightarrow K^0 + X$ final states. For $D_C^D(z')$ we have tried both a constant form and an exponential, $e^{-3z'}$, which were suggested by Lai²⁰ to provide a reasonable description of previous dilepton data. For the $D(1860) \rightarrow K^0 + X$ branching ratios the existing experimental data²¹ supplemented by theoretical predictions²² have been used. Finally, we have used phase space calculations for D meson decays into K^0 's.

Results of the above model, modified to meet our experimental conditions and the antineutrino energy spectrum, are shown in Fig. 5 where we present the K^0 mean multiplicity in current fragmentation region as a function of x (Fig. 5a) and y (Fig. 5b). The model predictions are shown with a flat charmed quark fragmentation

function (solid curve), with an exponential fragmentation function (dashed line) and without the assumption of charm production (dotted curve). The data have a strong predictive strength in the small x and high y regions and they are clearly inconsistent with the no-charm hypothesis. Because the statistics are limited we can not exclude either of the two charmed quark fragmentation functions, but there is an indication that the flat function describes the experimental data better.

3.4 Inclusive mass spectra

Using our results above, we should expect a rate of $\sim 6\%$ for charmed particle production in $\bar{\nu}N$ interactions. Therefore, it might be possible to see signals from charmed particle production in the effective mass distributions. A large number of competing charmed particle decay modes could, on the other hand, dilute the signal in any separate decay mode as well as the combinatorics in the high multiplicity events. We have searched for evidence of D^- and \bar{D}^0 production in the inclusive K^0 sample by studying the relevant invariant mass distributions.

The $K^0\pi^-$ invariant mass spectrum is shown in Fig. 6a. No signal is apparent near the $D^-(1868)$ mass in this distribution. A background estimation by a polynomial fit resulted in the following upper limit for the $D^-(1868)$ production in CC interactions:

$$\frac{\bar{\nu}N \rightarrow \mu^+ D^- X, D^- \rightarrow K^0 \pi^-}{\bar{\nu}N \rightarrow \mu^+ X} < 0.2\% \text{ (90\% c.l. upper limit)}$$

The $K^0 \pi^+ \pi^-$ effective mass distribution is presented in Fig. 7. There is no apparent signal from the $\bar{D}^0(1863)$ decays. Using the same procedure for background estimation as before we obtain the following upper limit for $\bar{D}^0(1863)$ production:

$$\frac{\bar{\nu}N \rightarrow \mu^+ \bar{D}^0 X, \bar{D}^0 \rightarrow K^0 \pi^+ \pi^-}{\bar{\nu}N \rightarrow \mu^+ X} < 0.3\% \text{ (90\% c.l. upper limit)}$$

Both these results may be compared with the D^+ and D^0 rates obtained in νN interactions: $0.1 \pm 0.1\%$ for D^+ production² and $0.40 \pm 0.15\%$ for D^0 production^{2,3}, respectively. By using the previously measured $D^- \rightarrow K^0 \pi^-$ and $\bar{D}^0 \rightarrow K^0 \pi^+ \pi^-$ branching ratios^{2,1} of $\sim 1.5\%$ for D^- and $\sim 4.4\%$ for \bar{D}^0 we obtain the upper limits of $\sim 13\%$ for total D^- production and $\sim 7\%$ for total \bar{D}^0 production in antineutrino-nucleon charged current interactions.

The $K^0 \pi^-$ and $K^0 \pi^+$ invariant mass distributions are presented in Fig. 6a,b. A signal from the $K^{*-}(890)$ production is seen (Fig. 6a) but no evidence for K^{*+} is seen (Fig. 6b). To get an estimate for the $K^{*-}(890)$ production rate we simulate non-resonant $K^0 \pi^-$ background by randomly associating K^0 mesons with negative pions from different events which were required to have approximately the same hadronic energy as the K^0 event. The resulting background distribution was normalized to the $K^0 \pi^-$ mass spectrum in the mass region outside the K^{*-} -mass (solid curve in Fig. 6). The following inclusive production rate for $K^{*-}(890) \rightarrow K^0 \pi^-$ in CC $\bar{\nu}N$ interactions was obtained:

$$\frac{\bar{\nu}N \rightarrow \mu^+ K^{*-}(890) + X, K^{*-} \rightarrow K^0 \pi^-}{\bar{\nu}N \rightarrow \mu^+ + X} = (0.81 \pm 0.34) \%$$

This value is close to the $K^{*-}(890)$ production rate obtained in neutrino interactions²³.

The effective mass distributions for the combination $\Lambda\pi^-$ and $\Lambda\pi^+$ are shown in Fig. 8a and Fig. 8b respectively. We observe a strong signal from the $\Sigma^-(1385)$, but there is no indication of the $\Sigma^+(1385)$ in the $\Lambda\pi^+$ mass spectrum. This behaviour is also observed in $\bar{\nu}p$ interactions⁷ and the opposite to that is seen in νp reactions¹². By using the same procedure for determination of non-resonant background we obtained the inclusive $\Sigma^-(1385) \rightarrow \Lambda\pi^-$ yield in $\bar{\nu}N$ CC interactions of

$$\frac{\bar{\nu}N \rightarrow \mu^+ \Sigma^-(1385) + X, \Sigma^- \rightarrow \Lambda\pi^-}{\bar{\nu}N \rightarrow \mu^+ + X} = (0.30 \pm 0.19) \%$$

which is again in a good agreement with the $\Sigma^+(1385)$ production rate obtained in neutrino reactions²³.

Taking into account our data on the K^0 and Λ inclusive production rates we obtain that only $5 \pm 2\%$ of the K^0 mesons and Λ hyperons results from the decays of $K^{*-}(890)$ and $\Sigma^-(1385)$ resonances, respectively.

3.5 K^0 and Λ production on proton and neutron targets

The study of neutral strange particle production in anti-neutrino interactions on proton and neutron targets separately can add to our understanding of the di-quark fragmentation processes and the nucleon structure. Measurements of the Λ production are particularly important because Λ hyperons are the only baryons which can be identified with a high efficiency. Moreover, almost all Λ 's are produced in the target fragmentation region⁸.

Separation of the V^0 production off a proton and neutron target is based on the total final state charge. The details of this separation procedure have been described elsewhere². This method gives the following results:

$$\langle n_K^p \rangle = 0.18 \pm 0.02; \quad \langle n_K^n \rangle = 0.11 \pm 0.02$$

$$\langle n_\Lambda^p \rangle = 0.07 \pm 0.01; \quad \langle n_\Lambda^n \rangle = 0.05 \pm 0.01$$

where $\langle n_{K(\Lambda)}^{p(n)} \rangle$ is the average multiplicity of K^0 mesons (Λ hyperons) produced in $\bar{\nu}p$ ($\bar{\nu}n$) charged current interactions. The obtained results of K^0 and Λ production on the proton target are in a good agreement with the similar data obtained in $\bar{\nu}p$ interactions (see Table II).

In Fig. 9 we present the x_F dependence of the ratio $R_{p/n}^V$ for the K^0 's (Fig. 9a) and Λ 's (Fig. 9b) where x_F is the Feynman scaling variable $x_F = 2p_L^*/W$ and $R_{p/n}^V = \langle n_V^p \rangle / \langle n_V^n \rangle$. Here p_L^* is the hadron momentum along the current direction in hadron center-of-mass system. There is no significant dependence of this ratio versus x_F for both K^0 and Λ data. For the whole x_F interval we have the following results:

$$R_{p/n}^K = 1.60 \pm 0.32$$

$$R_{p/n}^\Lambda = 1.51 \pm 0.33$$

To remove possible quasi-elastic particle production we have made the selection $W^2 > 10 \text{ GeV}^2$. The results for the forward and backward c.m.s. hemispheres are shown in Table III. Within errors, the K^0 multiplicity is the same for the proton and neutron targets and for the forward and backward directions.

The experimental result for the Λ 's in the target fragmentation region ($x_F < 0$) is unexpected in the naive QPM because in $\bar{\nu}p$ CC interactions the spectator di-quark system consists of a (ud)-pair and in $\bar{\nu}n$ CC interactions of a (dd)-pair. Therefore, it should be easier to produce a Λ hyperon in $\bar{\nu}$ interactions off protons than off neutrons. Our result $R_{p/n}^\Lambda = 1.16 \pm 0.32$ for backward Λ 's does not agree with these qualitative expectations.

IV. SUMMARY

We have performed a detailed study of neutral strange particle production in charged current $\bar{\nu}N$ interactions. The major results can be summarized as follows:

- (1) The over-all yield of the CC events with neutral strange particles is 0.16 ± 0.01 . The inclusive K^0 and Λ production rates are 0.164 ± 0.009 and 0.063 ± 0.004 , respectively. The single Λ production is estimated to be $1.1 \pm 0.7\%$.
- (2) The W^2 dependence of average K^0 and Λ multiplicity is well described by a logarithmic form $(a+b \cdot \ln W^2)$ or a power-law relation $(a+bW^{1/2})$. We see no significant Q^2 dependence of $\langle n_V \rangle$ in the regions $W^2 < 20 \text{ GeV}^2$ and $W^2 > 20 \text{ GeV}^2$.
- (3) The average K^0 multiplicity does not depend on W^2 or Q^2 in the current fragmentation region ($z > 0.3$).
- (4) In the QPM framework our V^0 data are consistent with the charm hypothesis. Fitting $\langle n_V \rangle$ as functions of x and y , the K^0 and Λ multiplicity from the charmed particle decays is found to be $6 \pm 2\%$. This result is consistent with dilepton data obtained in this experiment.
- (5) The K^0 data in the high z region ($z > 0.3$) are in agreement with the QPM predictions with a flat charmed quark fragmentation function.

- (6) The upper limits for $D^- \rightarrow K^0 \pi^-$ and $\bar{D}^0 \rightarrow K^0 \pi^+ \pi^-$ production rates are estimated to be 0.2% and 0.3%, respectively.
- (7) There are signals from $K^{*-}(890)$ and $\Sigma^-(1385)$ resonances in the effective mass spectra. The observed relative yields are $0.81 \pm 0.34\%$ for $K^{*-} \rightarrow K^0 \pi^-$ and $0.30 \pm 0.19\%$ for $\Sigma^- \rightarrow \Lambda \pi^-$ which are in an agreement with the K^{*+} and Σ^+ rates obtained in neutrino interactions.
- (8) The ratios between K^0 's produced off proton and neutron targets in the $W^2 > 10 \text{ GeV}^2$ region are 1.26 ± 0.49 ($x_F < 0$) and 1.49 ± 0.37 ($x_F > 0$). The value of this ratio for backward Λ 's is 1.16 ± 0.32 , and does not agree with expectations derived from the naive QPM.

ACKNOWLEDGEMENTS

We wish to thank the members of the Neutrino Laboratory at Fermilab and the scanning, measuring and secretarial staffs at our respective laboratories for their contribution to this experiment. This work was supported in part by the U.S. Department of Energy and the National Science Foundation.

REFERENCES

- ¹ S.L. Glashow, J. Iliopoulos, L. Maiani, Phys. Rev. D2 (1970) 1285.
- ² G.F. Feldman et al., Phys. Rev. Lett. 38 (1977) 1313.
R.W. Brandelik et al., Phys. Lett 70B (1977) 132.
M. Piccolo et al., Phys. Lett. 70B (1977) 260.
G. Goldhaber et al., Phys. Rev. Lett. 37 (1976) 255.
I. Peruzzi et al., Phys. Rev. Lett. 37 (1976) 569.
- ³ B. Knapp et al., Phys. Rev. Lett. 37 (1976) 882.
M.S. Atiyà et al., Phys. Rev. Lett. 43 (1979) 414.
- ⁴ C. Baltay et al., Phys. Rev. Lett. 41 (1978) 73.
C. Baltay et al., Phys. Rev. Lett. 42 (1979) 1721.
- ⁵ J.P. Berge et al., Phys. Lett. 81B (1979) 89.
- ⁶ R.P. Feynman, Photon-Hadron Interactions (W.A. Benjamin, Reading, Massachusetts, 1972).
- ⁷ V.E. Barnes, Strange Particle Production in $\bar{\nu}p$ Interactions, Proc. of the Int. Conference "Neutrino 79", Bergen, 1979, V.2, 582.
- ⁸ V.V. Ammosov et al., Nucl. Phys. B162 (1980) 205.
- ⁹ D. Sinclair, Measurement of x and y Distributions for Anti-neutrino Charged Current Inelastic Scattering, Proc. of the Int. Conference "Neutrino 79", Bergen, 1979, V.2, 343.

- ¹⁰This method has been described in Ref. 9. Here we use a slightly modified procedure: the parameters a and b in the formula P_X^H (corrected) = $a + bP_X^H(\text{visible})$ were considered as functions of the transverse momentum imbalance in each event, P_T/P_X , where P_T and P_X are the transverse and longitudinal total momenta of the event with respect to the incident antineutrino direction.
- ¹¹R.B. Palmer, Lepton and Charm Production in the 15-Ft. Bubble Chamber, Proc. of the XIII Rencontre de Moriond, Les Arcs-Savoie, 1978 (28100 DREUX, France, 1978) V.2, 361.
- ¹²J.P. Berge et al., Phys. Rev. D18 (1978) 1359.
- ¹³M. Derrick et al., Phys. Rev. D17 (1978) 17.
- ¹⁴R. Orava, ABCMO νp data, private communication.
- ¹⁵L. Pape, Estimation of Charm Production and Lifetime Limits in ν Interactions at BEBC, Proc. of the Topical Conf. on Neutrino Physics at Accelerators, Oxford, 1978 (Pub. RL-78-081) 167.
- ¹⁶B. Cork and T.F. Hoang, Multiplicity and Scaling of $e^+e^- \rightarrow$ hadrons, preprint LBL-9958, 1979.
- ¹⁷R.D. Field and R.P. Feynman, Phys. Rev. D15 (1977) 2590.
R.D. Field and R.P. Feynman, Nucl. Phys. B136 (1978) 1.
- ¹⁸We have used the following values for the parameters a and b : $a = -0.005$, $b = 0.0175$ given in F. Messing, Strange Particle Production in Lepton Proton Interactions, Proc. of the Topical Conf. on Neutrino Physics at Accelerators, Oxford, 1978 (Pub. RL-78-081) 26.

- ¹⁹I. Cohen et al., Phys. Rev. Lett. 40 (1978) 1614.
- ²⁰C.-H. Lai, Phys. Rev. D18 (1978) 1422.
- ²¹Review of Particle Properties, Phys. Lett. 75B (1978).
- ²²C. Quigg and J.L. Rosner, Phys. Rev. D17 (1978) 239.
- ²³P. Schreiner, Particle Production by Neutrinos, Proc. of the Int. Symposium on Lepton and Photon Interactions at High Energies, Fermilab, 1979, 291.
- ²⁴J.P. Berge et al., Phys. Lett. 84B (1979) 511.

TABLE I
OBSERVED AND CORRECTED NUMBER OF CHARGED
CURRENT EVENTS WITH NEUTRAL STRANGE PARTICLES.

CHANNEL	OBSERVED EVENTS	CORRECTED EVENTS	PRODUCTION RATE
$\bar{\nu}_N \rightarrow \mu^+ K^0 X$	276	448 ± 125	0.055 ± 0.015
$\bar{\nu}_N \rightarrow \mu^+ \Lambda X$	229	301 ± 42	0.037 ± 0.005
$\bar{\nu}_N \rightarrow \mu^+ \bar{\Lambda} X$	7	16 ± 5	0.002 ± 0.001
$\bar{\nu}_N \rightarrow \mu^+ K^0 \bar{K}^0 X$	23	343 ± 71	0.042 ± 0.009
$\bar{\nu}_N \rightarrow \mu^+ \Lambda K^0 X$	28	212 ± 40	0.026 ± 0.005
$\bar{\nu}_N \rightarrow \mu^+ V^0 X$	563	1320 ± 79	0.162 ± 0.010

TABLE II
COMPARISON OF THE INCLUSIVE STRANGE PARTICLE
PRODUCTION RATES IN DIFFERENT ν AND $\bar{\nu}$ EXPERIMENTS.

Ref.	$R_K = N_{K^0}/N_{CC}$	$R_\Lambda = N_\Lambda/N_{CC}$	$R_{\Lambda/K} = N_\Lambda/N_{K^0}$
this exp.	0.16 ± 0.01	0.06 ± 0.01	0.38 ± 0.03
νN^{11}	0.14 ± 0.02	0.05 ± 0.01	0.37 ± 0.06
νp^{12}	0.14 ± 0.02	0.06 ± 0.02	0.40 ± 0.11
$\bar{\nu} p^{13}$	0.15 ± 0.04	0.06 ± 0.02	0.40 ± 0.16
νp^{13}	0.15 ± 0.02	0.04 ± 0.01	0.30 ± 0.07

TABLE III
NEUTRAL STRANGE PARTICLE PRODUCTION ON PROTON
AND NEUTRON TARGET, $W^2 > 10 \text{ GeV}^2$.

$R_{p/n}^V = \langle n_V^P \rangle / \langle n_V^n \rangle$	$x_F < 0$	$x_F > 0$ *)
$R_{p/n}^K$	1.26 ± 0.49	1.49 ± 0.37
$R_{p/n}^\Lambda$	1.16 ± 0.32	-

*) Our statistics do not allow us to give a result for
the Λ 's in the region $x_F > 0$.

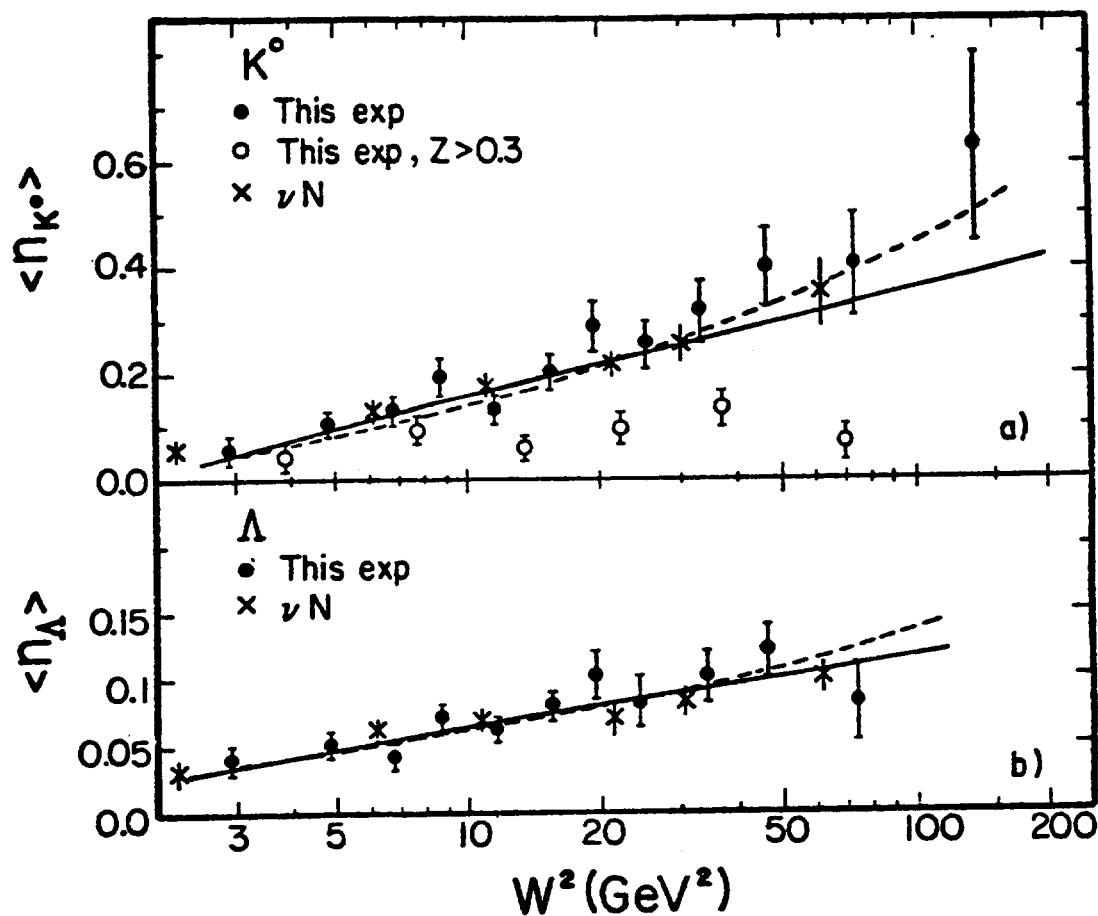


FIG. 1

Fig. 1: Average multiplicity of K^0 's (a) and Λ 's (b) as a function of W^2 . Solid and dashed lines represent the results of the logarithmic and power-law fits, respectively, described in the text. The neutrino-nucleon data are also shown. The open data points give K^0 multiplicity in the region $z > 0.3$.

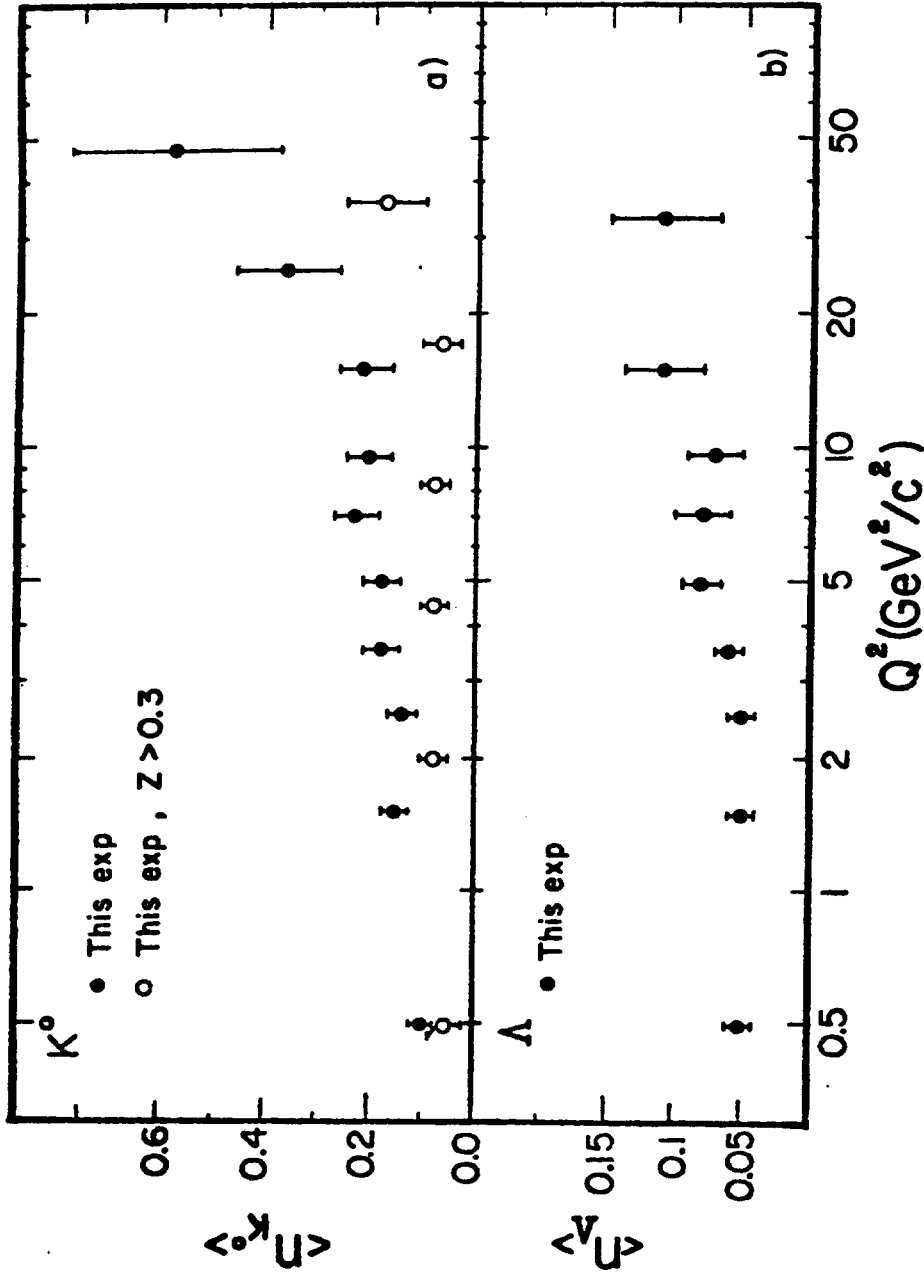


FIG. 2

Fig. 2: Average multiplicity of K^0 's (a) and Λ 's (b) as a function of Q^2 . Open data points represent the K^0 data in the current fragmentation region $z > 0.3$.

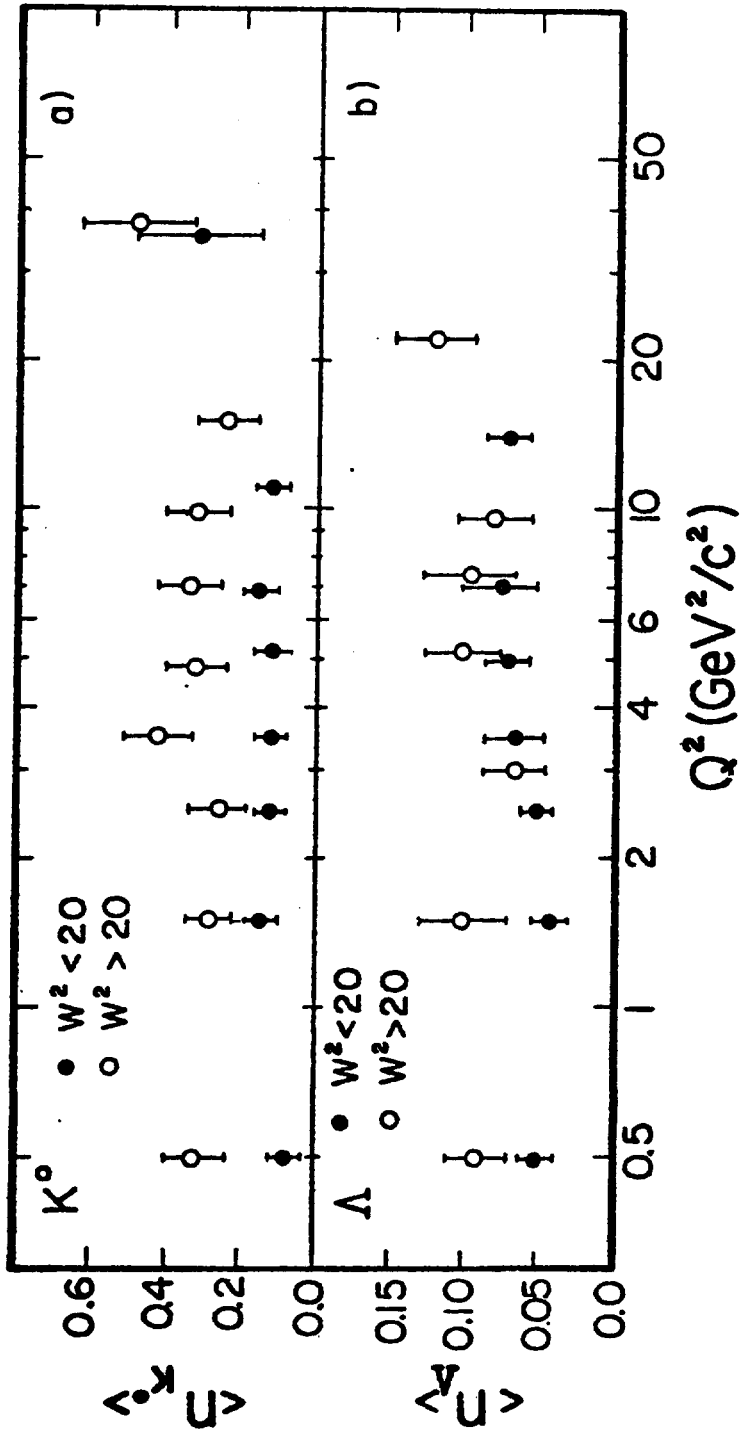


FIG. 3

Fig. 3: Q^2 dependence of the mean multiplicity of the K^0 's (a) and Λ 's (b). The black data points show the multiplicities in the low W^2 region ($< 20 \text{ GeV}^2$), the open data points give the data in high W^2 region ($> 20 \text{ GeV}^2$).

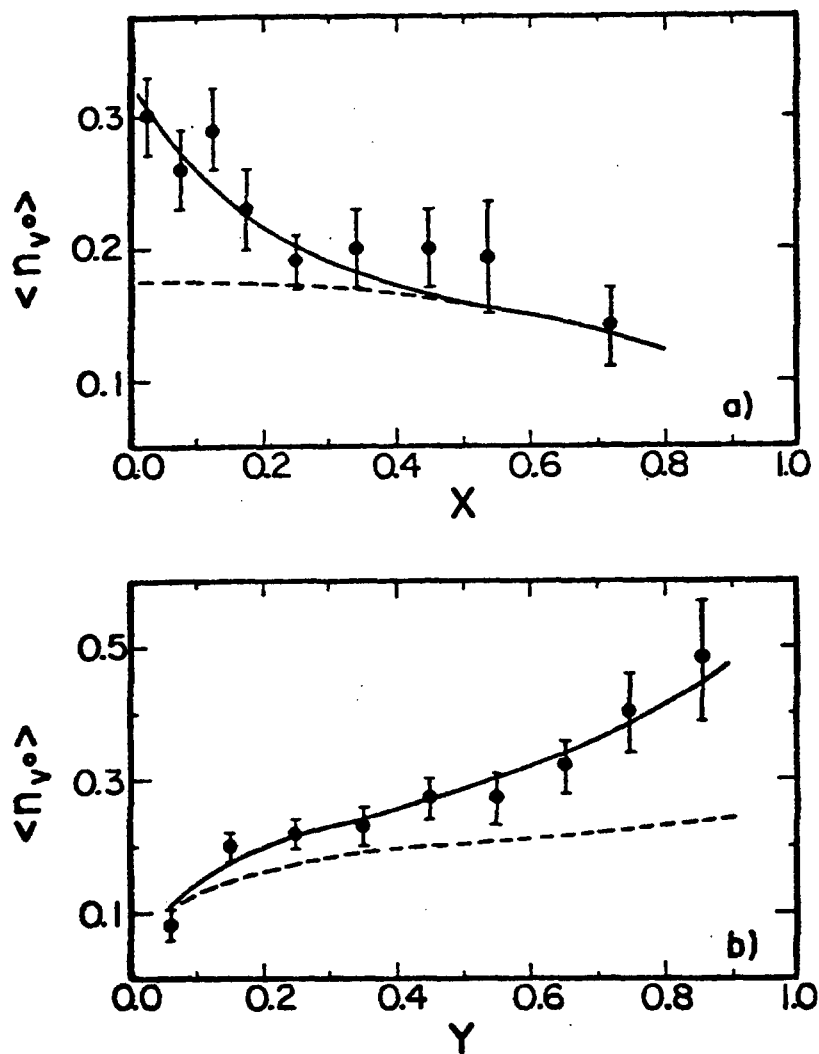


FIG.4

Fig. 4: Mean multiplicity of V^0 's (K^0 's and Λ 's) as a function of x (a) and y (b). Solid curves result from the fit with the charm term (see the text). Dashed lines show the non-charm part of this fit.

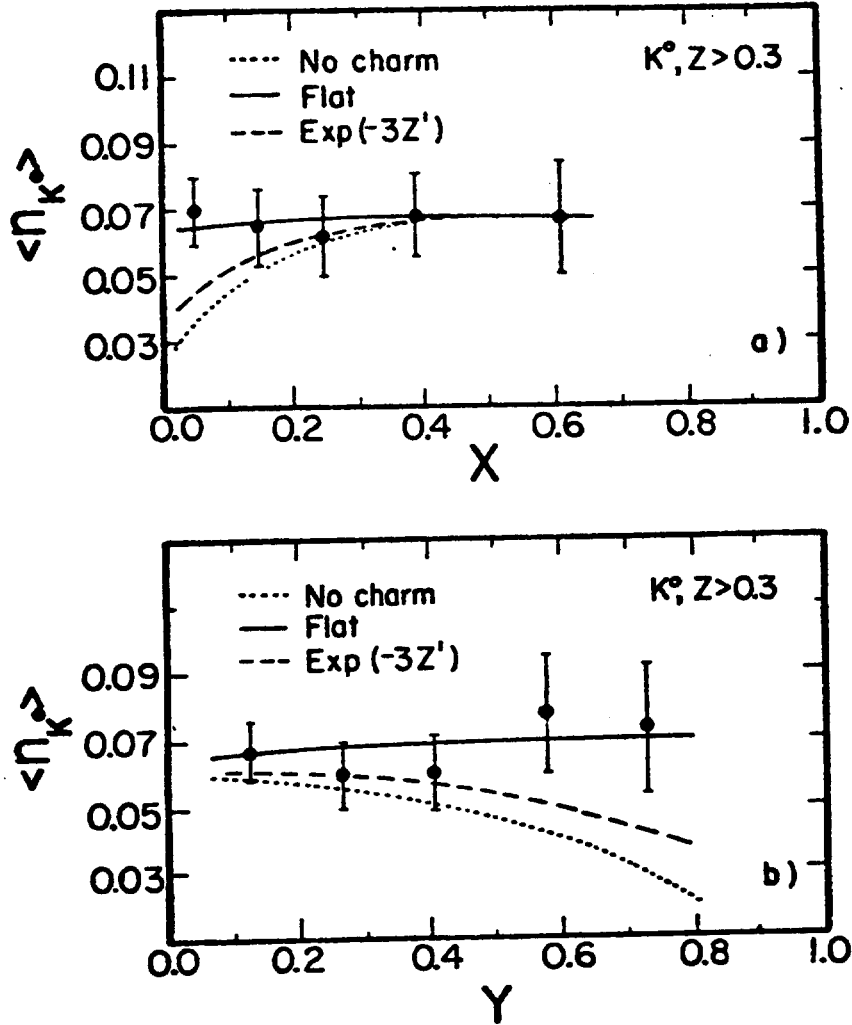


FIG. 5

Fig. 5: The x (a) and y (b) dependences of the K^0 mean multiplicity in the current fragmentation region $z > 0.3$. Dotted lines represent the QPM predictions without charm, dashed lines give the predictions with an exponential charmed quark fragmentation function and solid lines with a flat charmed quark fragmentation function (see the text).

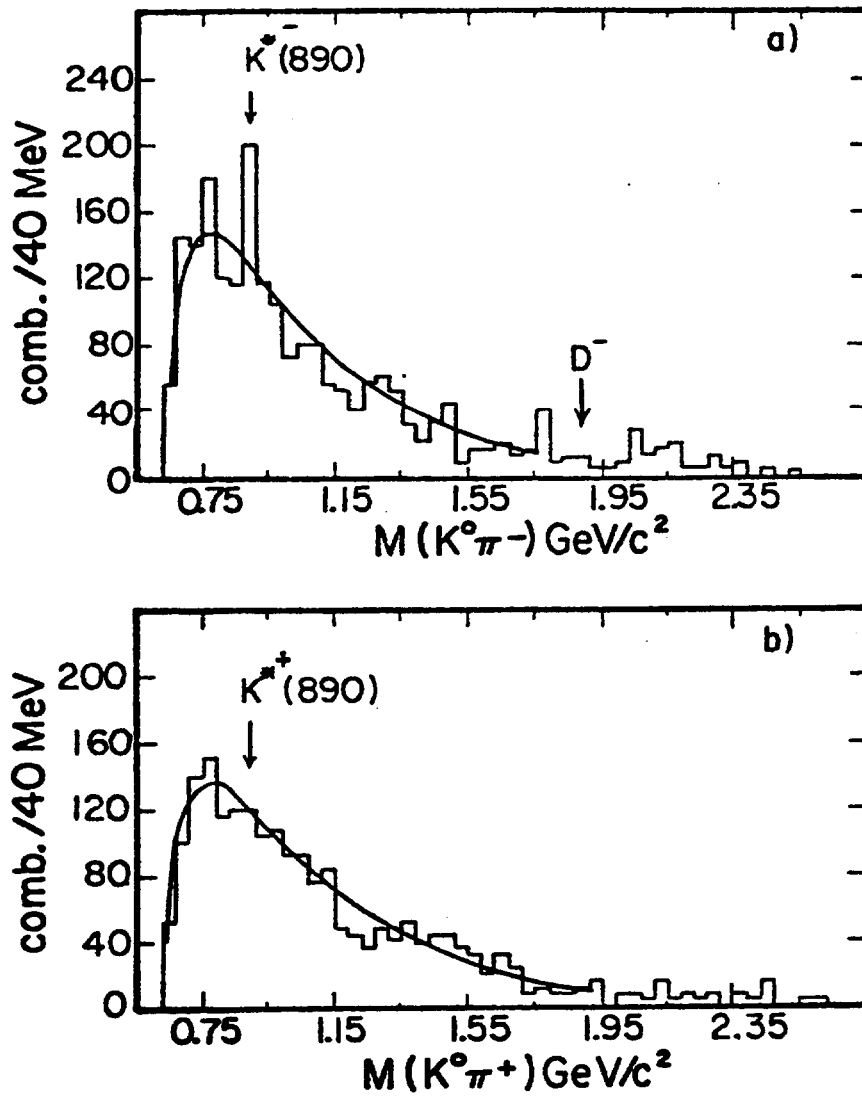


FIG. 6

Fig. 6: The invariant mass distribution for $K^0\pi^-$ (a), $K^0\pi^+$ (b). An estimate of the background is shown by the solid curve. In Fig. 6, 7 and 8 weighted combinations are presented.

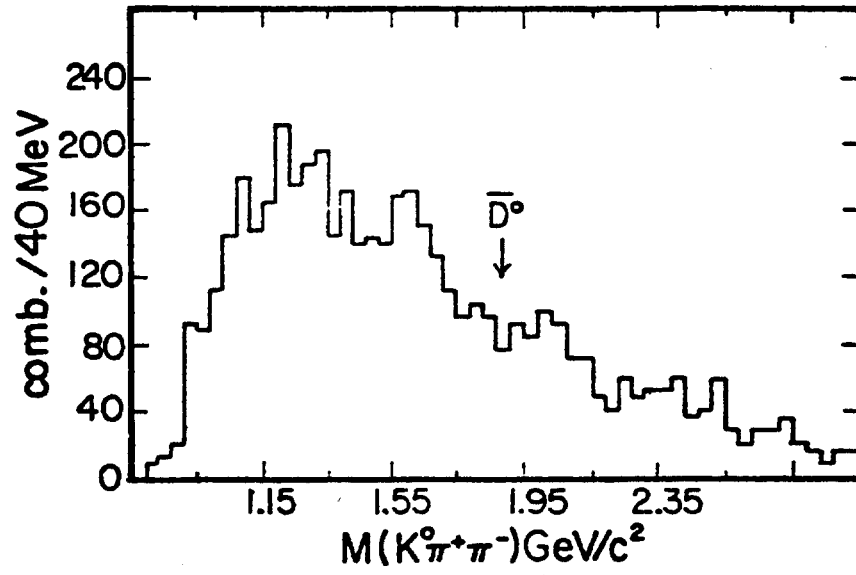


FIG. 7

Fig. 7: The $K^0 \pi^+ \pi^-$ invariant mass distribution.

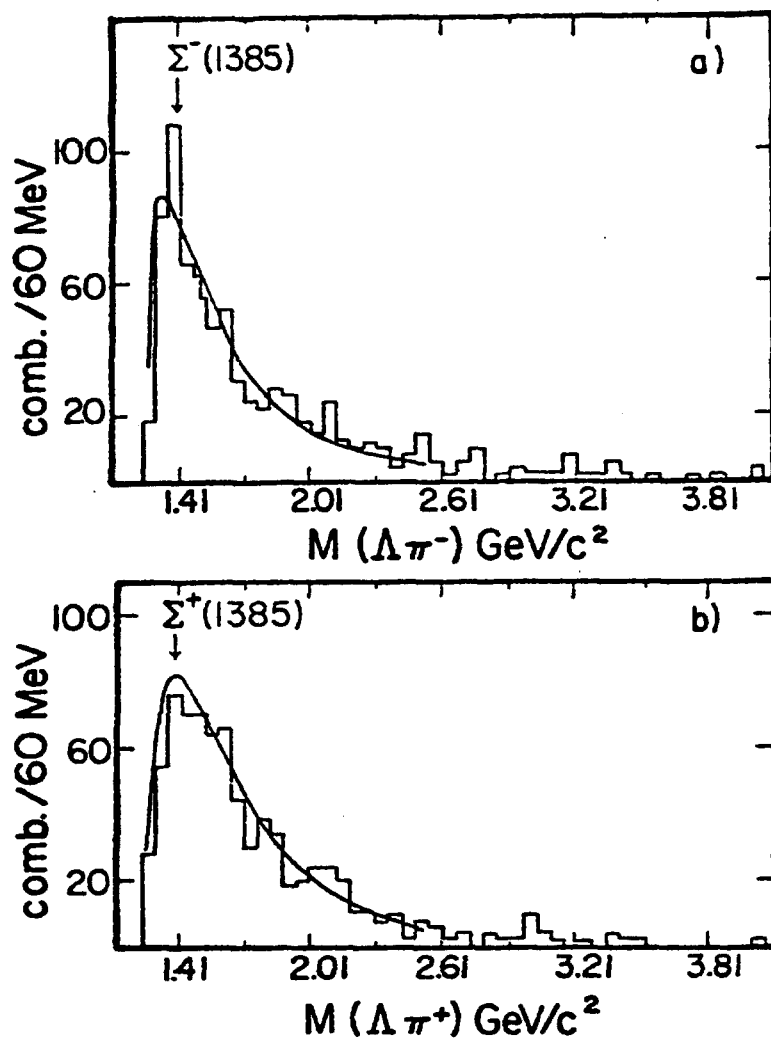


FIG. 8

Fig. 8: The effective mass spectrum for $\Lambda \pi^-$ (a), $\Lambda \pi^+$ (b). The solid curve represents the estimated background.

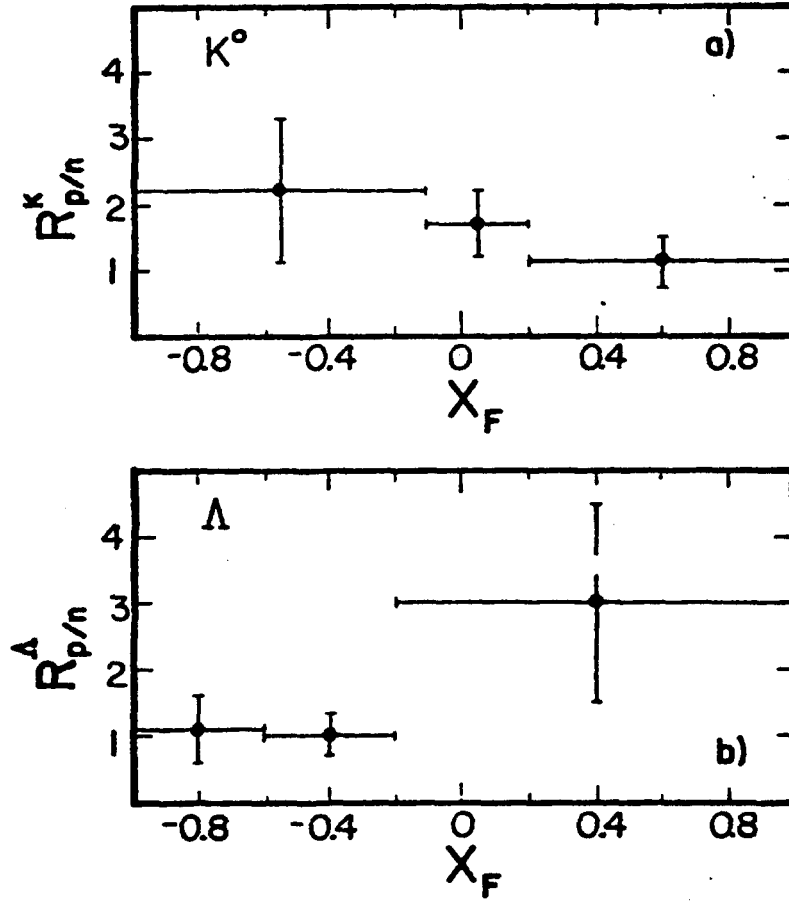


FIG. 9

Fig. 9: Relative production rates of K^0 's(a) and Λ 's(b) from CC interactions off proton and neutron targets as a function of x_F .